Comparative FTR- and Ramanspectroscopic Studies of Fundamental Mode Frequencies in $LiNbO_2$ and the Present Limit of Oblique Phonon Dispersion Analysis

E. Schuller, R. Claus, and H. J. Falge

Sektion Physik der Universität München, Lehrstuhl J. Brandmüller, Schellingstraße 4, 8000 München

G. Borstel

Fachbereich Physik der Universität Münster, 4400 Münster

(Z. Naturforsch. **32 a**, 47–53 [1977]; received November 27, 1976)

The assignments of fundamental mode frequencies in $LiNbO_3$ determined by IR- and Raman scattering-experiments show some characteristic differences. Comparative frustrated total reflection (FTR)- and Raman scattering-studies were carried out in order to find the origin of these discrepancies. The most serious deviation was due to the fact that in one case the ordinary phonon is observed by Raman scattering whereas the extraordinary mode is recorded only by FTR. It has been shown, on the other hand, that the oblique phonon dispersion technique did not provide arguments for the correct assignments. The main limit of the method is due to the fact that the influence of exciton states on polaritons hitherto is taken into account only by a constant high frequency dielectric 'function' (ε_∞). The uncertainty in the choice of a suitable ε_∞-value allows fittings of quite diverging sets of experimentally determined fundamental frequencies.

Introduction

The dependence of phonon frequencies on the wave vector direction in polar crystals is derived from the macroscopic phonon-polariton theory in the limit of large wave vector magnitudes. It quantitatively yields in uniaxial crystals

$$\sin^2\Theta \times \varepsilon_\perp^\infty \prod_{i=1}^{n_\perp} (\omega_{\perp \mathrm{L}i}^2 - \omega^2) \prod_{j=1}^{n_\parallel} (\omega_{\parallel \mathrm{T}j}^2 - \omega^2) + \cos^2\Theta \times \varepsilon_\parallel^\infty \prod_{j=1}^{n_\parallel} (\omega_{\parallel \mathrm{L}j}^2 - \omega^2) \prod_{i=1}^{n_\perp} (\omega_{\perp \mathrm{T}i}^2 - \omega^2) = 0\,, \quad (1)$$

see e. g. [1]. Θ denotes the angle between the wave vector direction and the optic axis, $\varepsilon_\perp^\infty$ and $\varepsilon_\parallel^\infty$ are the "high frequency dielectric constants" for electric field polarizations perpendicular and parallel to this axis, and the $\omega_{\mathrm{L}i}$ and $\omega_{\mathrm{T}i}$ are longitudinal and transversal fundamental mode frequencies. They are recorded for large wave vectors propagating parallel or perpendicular to the optic axis. The frequencies of totally symmetric modes with lattice displacements parallel to this axis are indicated by a subscript $\parallel$ and twofold degenerate modes with polarizations lying in the optically isotropic plane by $\perp$. $n_\parallel$ and $n_\perp$ correspondingly are the number of modes in both cases.

Reprint requests to Dr. Reinhart Claus, Sektion Physik (Experimentalphysik) der Universität München, Schellingstraße 4/IV, *D-8000 München 40*.

It is well known that the determination of the fundamental frequencies may in principle be achieved by simple well defined light scattering or infrared reflection measurements [2–4]. It is well known too, however, that weak scattering intensities and small oscillator strengths may cause great difficulties especially in "more than two atomic"-crystals. As a result the number of polyatomic crystals with a complete assignment of the fundamental phonon spectrum still is surprisingly small. The importance of such assignments is obvious. Numerical lattice dynamical calculations of different crystal properties frequently start from this level because force constants usually are still less known. Detailed measurements of the phonons directional dispersion therefore showed to be a very helpful tool in the view of this aspect [5, 6]. From Eq. (1) it can be seen that an experimental fit of isolated directional dispersion branches is not possible in an arbitrary way because other branches which might be unambiguously verified are always influenced by such a procedure. In the case of $LiNbO_3$ Claus and coworkers in 1972 could refine wave numbers given earlier in the literature and correct some errors which hardly would have been detected otherwise. Although $LiNbO_3$ nowadays is supposed to be one of the most well known crystals recent measurements of the phonon directional dependence by an infrared reflection technique showed deviations from the data

obtained by Raman scattering. These differences were shown to be specific for the different experimental methods. A comparison of experimental Raman- and IR-data of $LiNbO_3$ with calculated dispersion branches is used in the following to demonstrate the present limit of the directional dispersion analysis.

Results and Discussion

An infrared reflection technique to observe bulk phonons and polaritons has been described and demonstrated earlier on uniaxial α-quartz and $K_3Cu(CN)_3$ [1, 7–9]. In these references the reflection spectra were taken from samples being "principal cuts" i. e. the optic axes were arranged perpendicular to one of the surfaces, respectively. In a recent paper [10] the method has been generalized for arbitrary cuts where the optic axis forms an angle ϑ with the surface normal. The reflectivity $R_{TM}(\alpha, \vartheta, \omega)$ of a transverse magnetic (TM) incident wave being a function of the angle ϑ, frequency ω and the reflectance angle α becomes

$$R_{TM}(\alpha, \vartheta, \omega) = \left| \frac{\cos\alpha - (\omega/c)\, n\, B/C}{\cos\alpha + (\omega/c)\, n\, B/C} \right|^2, \quad (2)$$

where

$$B = (\varepsilon_{\parallel} \cos^2\vartheta + \varepsilon_{\perp} \sin^2\vartheta)\, k_z - (\varepsilon_{\parallel} - \varepsilon_{\perp})(\cos\vartheta \sin\vartheta)\, k_x$$

and

$$C = (\varepsilon_{\parallel} \cos^2\vartheta + \varepsilon_{\perp} \sin^2\vartheta)\, k_z^2 + (\varepsilon_{\parallel} \sin^2\vartheta + \varepsilon_{\perp} \cos^2\vartheta)\, k_x^2 - 2(\varepsilon_{\parallel} - \varepsilon_{\perp})(\cos\vartheta \sin\vartheta)\, k_x k_z .$$

The wave vector-component k_x of the incident ray depends on the reflectance angle α in the usual way [1, 9]

$$k_x = (\omega/c)\, n \sin\alpha . \quad (3)$$

n is the refractive index of the first medium [7]. The component k_z of the refracted wave in the second medium ist given explicitely by

$$k_z = \frac{(\varepsilon_{\parallel} - \varepsilon_{\perp}) \cos\vartheta \sin\vartheta}{\varepsilon_{\parallel} \cos^2\vartheta + \varepsilon_{\perp} \sin^2\vartheta} k_x \pm \frac{1}{\varepsilon_{\parallel} \cos^2\vartheta + \varepsilon_{\perp} \sin^2\vartheta} \cdot \sqrt{[k_x^2 - (\omega^2/c^2)(\varepsilon_{\parallel} \cos^2\vartheta + \varepsilon_{\perp} \sin^2\vartheta)]\,(-\varepsilon_{\parallel}\varepsilon_{\perp})} . \quad (4)$$

It can easily be verified that the reflectivity described by Eq. (2) reduces to the form earlier given in [7] and [8] for $\vartheta = 0°$ or $\vartheta = 90°$. Equation (4) becomes the well known dispersion relation of extraordinary bulk polariatons for $k_x = 0$ i. e. $\alpha = 0$

$$\frac{k_z^2 c^2}{\omega^2} = \frac{\varepsilon_{\parallel}\varepsilon_{\perp}}{(\varepsilon_{\parallel} \cos^2\vartheta + \varepsilon_{\perp} \sin^2\vartheta)} . \quad (5)$$

Only in this special geometry the angles Θ from Eq. (1) and ϑ in Eq. (2) are identical.

The main advantage of the IR-reflection technique (FTR) described above is that it allows a separate recording of extraordinary modes whereas corresponding Raman spectra are always mixed up by those of the ordinary modes. We illustrate this by the ideal back scattering geometries sketched in Figure 1. For $\Theta = 0°$ the wave vectors $\boldsymbol{k}$ of the

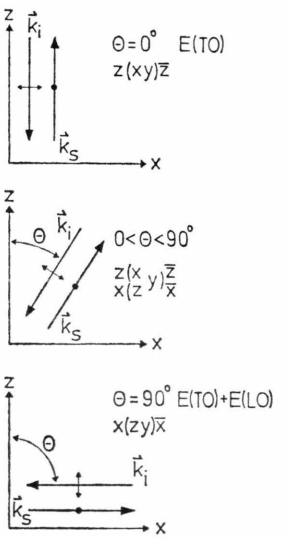

Fig. 1. Ideal back scattering geometries for different angles between the wave vectors and the optic axis (z). $\boldsymbol{k}_i$ and $\boldsymbol{k}_s$ describe the incident and scattered wave. The assumed polarization has been indicated on the arrows. Symbols for the scattering geometries are given in the usual way.

observed elementary excitations propagate parallel to the optic axis (z). The $\boldsymbol{k}$-direction is the same as that of $\boldsymbol{k}_i$. The polarization of the incident (i) and scattered (s) waves have been indicated by arrows and dots. Symbols for the scattering geometries are given in the well known way such as $z(xy)\bar{z}$. The Raman tensors element α_{xy} allows the observation of twofold degenerate models (E-modes). Their lattice displacements propagate in the optically isotropic plane and because $\boldsymbol{k} \parallel z$ there are only purely transverse modes for $\Theta = 0°$. For arbitrary values of Θ (center picture) Raman scattering occurs due to the two tensor elements α_{xy} and α_{zy} simultaneously. Both of them cause light scattering by E-modes. The degeneracy of the pairs of two linear independent TO-modes recorded for $\Theta = 0°$, however, is lifted now. One set of TO-modes with lattice

displacements lying in the xy-plane is left for all $\boldsymbol{k}$-directions. These are the ordinary E-modes. The others with linearly independent lattice displacements in the xz-plane are the extraordinary modes showing a mixed A_1- and E-character. Because Raman scattering takes place only due to the tensor elements α_{xy} and α_{zy} the E-components of their normal coordinates are recorded only. A spectra series corresponding to the different geometries shown in Fig. 1 is reproduced in Figure 2. The scans hardly

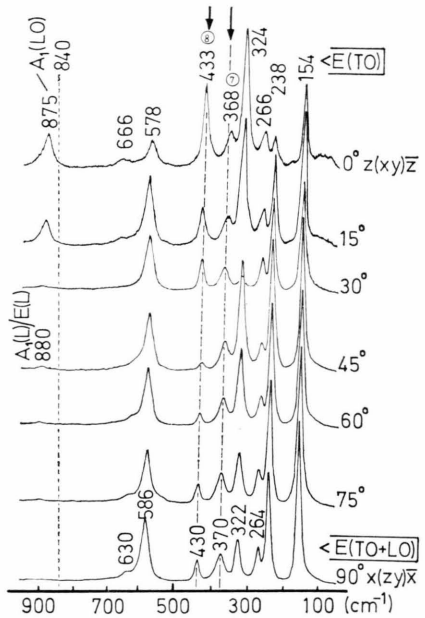

Fig. 2. Spectra series corresponding to the different scattering geometries in Figure 1. The scans mainly show the directionally independent ordinary phonons in $LiNbO_3$ see text.

show any frequency shifts of the phonons. This shows that light scattering from ordinary phonons is recorded mainly. Figure 3 shows a similar spectra series. $\Theta = 0°$, however, corresponds to $z(yy)\bar{z}$ in this case and if the wave vector triangles are arranged to lie in the xz-plane for all values of Θ Raman scattering occurs only due to the α_{yy}-element in all the spectra. α_{yy}-scattering allows the observation of A_1- as well as E-modes and consequently these spectra should mainly show the directional-dependent extraordinary phonons which in fact they do (see the Raman tensors of the $LiNbO_3$-factor group C_{3v} in e. g. Reference [1]).

Discrepancies appear on three directional dispersion branches when comparing the Raman- and IR-

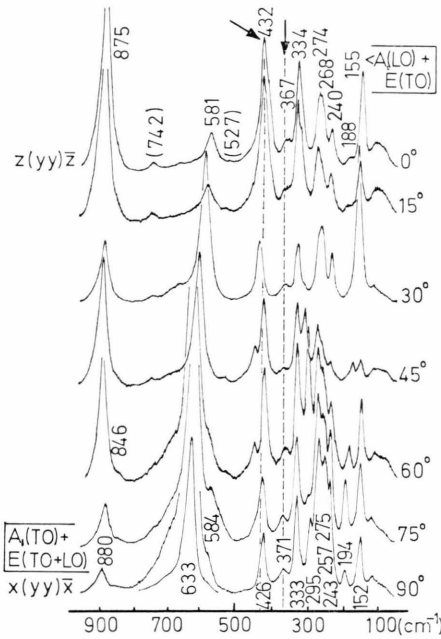

Fig. 3. Spectra series mainly showing the directional-dependent extraordinary phonon modes in $LiNbO_3$. All the scans are recorded due to the Raman tensor element α_{yy}.

data. Figure 4 shows the 13 dispersion branches of $LiNbO_3$ calculated on the basis of the Raman- (dotted curves) and infrared-date (full curves).

Branch Nr. 12 is predicted as an almost dispersion-free curve from the Raman spectra. The LO-TO-splitting of only 4 cm^{-1} from E (LO) 739 cm^{-1} to E (TO) 743 cm^{-1} is estimated from several spectra series. The branch is grouptheoretically determined to be polar and the mode strength thus should not vanish identically. Some of the corresponding Raman-lines can be identified in the spectra in Figure 3. Recent investigations of surface polariton dispersion in $LiNbO_3$ by Yakovlev and coworkers [11] seemed to show agreement with this assignment of branch nr. 12. Our own corresponding experiments, however, were not able to confirm the Raman data. Figure 5 shows two spectra series of the extraordinary surface polaritons in the region. The reflection geometry in A was the following. The optical axis (z) of the sample was perpendicular to the surface. The x-direction being the wave propagation direction was perpendicular to z and of course parallel to the surface. In the geometry B on the other hand the optical axis was lying in the surface and parallel to the wave propagation. A KRS 5-hemi-

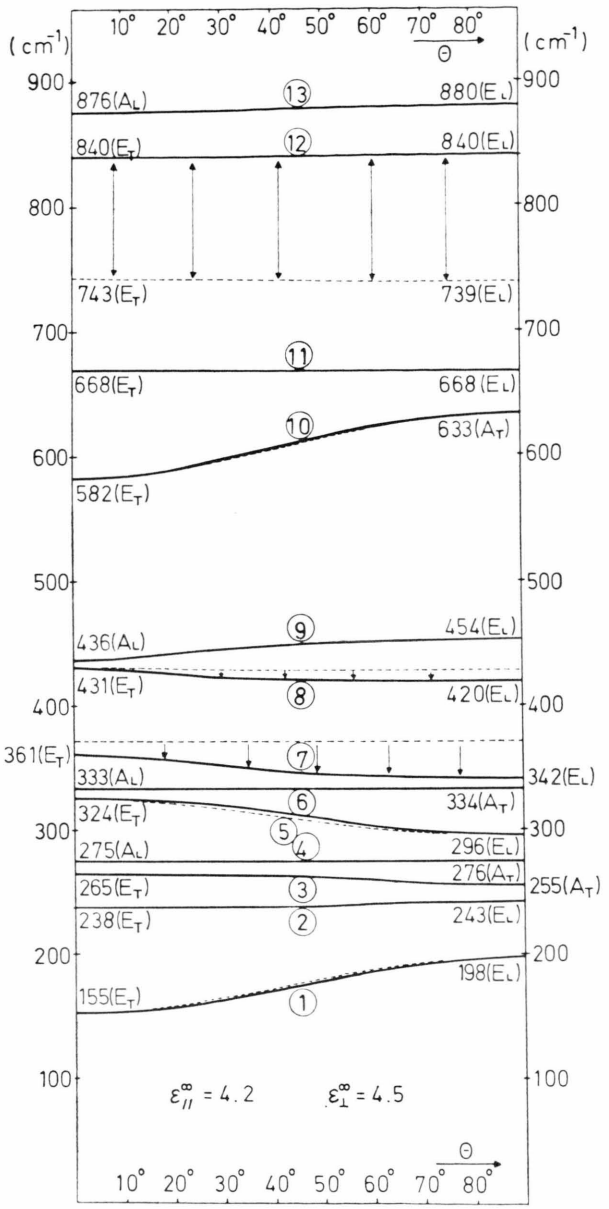

Fig. 4. Directional dispersion branches of the polar phonons in $LiNbO_3$. Full curves are calculated essentially on the basis of the infrared data and dashed curves on the basis of the Raman data.

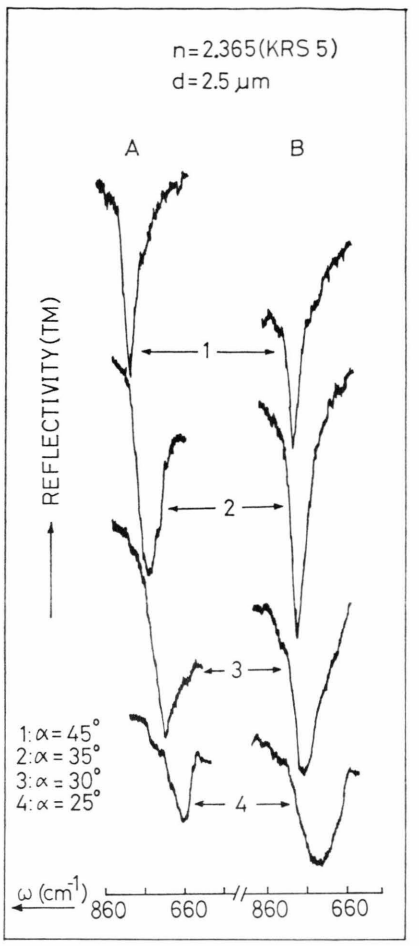

Fig. 5. Two spectra series of extraordinary surface polaritons in the higher frequency phonon region of $LiNbO_3$. For explanations, see text.

cylinder at a distance $d = 2.5\ \mu m$ from the sample was used as the ATR-medium. Variation of the refectance angle α allowed a variation of the magnitude of the wave vector component parallel to the surface in the usual manner, see [10]. The incident radiation was polarized transverse magnetically in both experiments. We point out that the band of reduced reflectivity in both cases crosses the position of the assumed polar E-branch at about 740 cm^{-1} without showing only a hint of a reflection maximum which should necessarily appear from theory. Figure 6 shows another two reflection spectra of the region [9, 12]. Scan A represents the conventional reststrahlen reflection spectrum recorded for $\alpha = 24°$. The optic axis of the sample was perpendicular to the surface and the incident radiation was polarized transverse electrically. B shows the ordinary surface polariton spectrum recorded for $\alpha = 35°$ and $d = 0.7\ \mu m$ when again using a KRS 5-hemicylinder. In none of the spectra there is an indication of the branch at $\sim 740\ cm^{-1}$ which was observed in the Raman-spectra, Figure 3. On the contrary the spectra in Fig. 6 obviously show a reflection minimum in the region slightly below

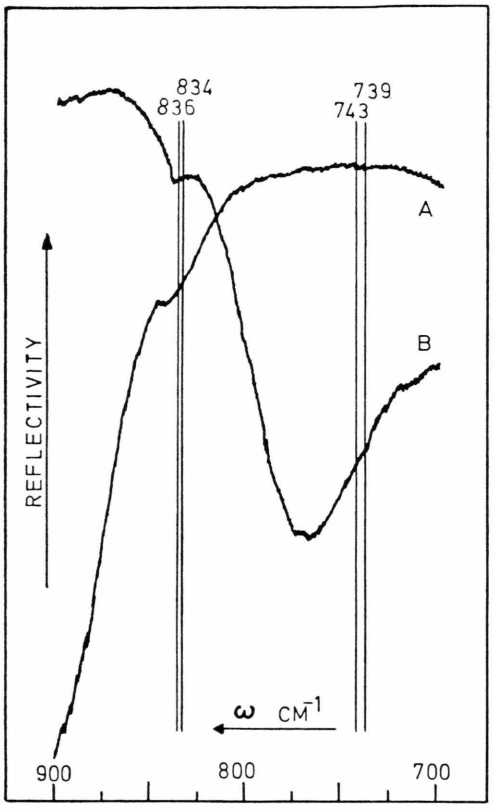

Fig. 6. Reststrahlenbands and ordinary polaritons in the higher frequency phonon region of $LiNbO_3$. A: TE-reflection spectrum for $\alpha=24°$, optic axis $z \perp$ surface. B: ordinary surface polaritons for $\alpha=35°$, ATR-crystal=KRS 5 and $d=0.7$ μm see text.

850 cm^{-1}. These bands allow the assignment of two phonons: E (LO) 834 and E (TO) 836 cm^{-1}. The IR-spectra thus suggest a first order polar mode in this region. A comparison with the Raman data shows that a very weak signal at ~ 846 cm^{-1} in the $\Theta=60°$ spectrum possibly might coincide with these infrared bands. The decision which of the two phonon couples is the first order polar mode cannot be achieved from our experiments. The pair E(LO) 739/E(TO) 743 cm^{-1} might be of first order but the LO-TO-splitting and consequently the mode strength could be much weaker so that an observation in the IR-spectra is impossible. Then the pair E(LO) 834/E(TO) 836 cm^{-1} most probably corresponds to a second order process. The reverse situation, however, might be true as well. Directional dispersion measurements do not help to decide the question because both branches are almost flat, see Figure 4. They do not give a significant contribution to the Lyddane-Sachs-Teller ratio and thus do not affect the other dispersion branches.

We now turn our attention to the lower frequency region. From Eq. (2) we can determine which areas in the ω/k-diagram correspond to transparency and which to reflectivity. The two typs of areas are separated by the dispersion curves of bulk polaritons. In real reflection spectra the turning points of the edges of the reflection bands, correspond to points on the polariton curves, see [1, 7–9]. Figure 7

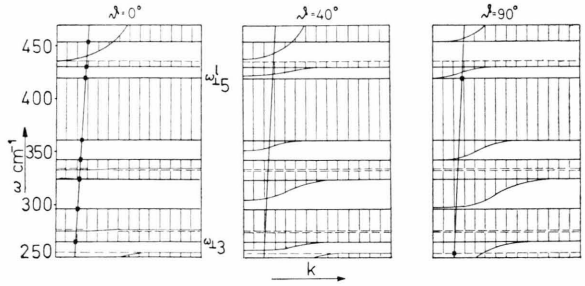

Fig. 7. Qualitative ω/k-diagrams of $LiNbO_3$ for $\vartheta=0°$, 40° and 90° between the surface normal and the optic axis. Hatched areas correspond to full reflection, whereas the others correspond to transparency. The straight lines with squares show the traces which correspond to the reflection spectra in Figure 8.

shows three ω/k-diagrams for different values of the angle ϑ between the optic axis (z) and the surface normal of the sample. Corresponding reflection experiments as shown in Fig. 8 allow the determination of polariton directional dispersion from IR-spectra. The traces in Fig. 7 directly correspond to the three spectra in Figure 8. The squares are added in both figures in order to allow a better orientation.

A minor discrepancy between the Raman spectra and IR-measurements on the basis of the reflection method described above can be seen on branch nr. 8 in Figure 4. The phonon assignment derived from light scattering experiments was E(LO) 428/E(TO) 431 cm^{-1}. The IR-measurements, however, suggest E(LO) 420/E(TO) 431 cm^{-1}. The frequency splitting thus is enlarged from ~ 3 to ~ 11 cm^{-1}. We believe that this is still within the experimental error when taking into account the different influence of the line half widths in the Raman- and IR-spectra. The wave numbers given earlier [5] were averaged from a number of directional dispersion

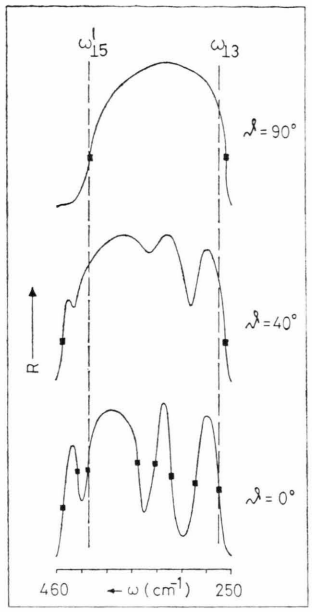

Fig. 8. Reflection spectra of three samples of $LiNbO_3$. The optic axis, respectively, forms the angles $\vartheta = 0°$, 40° and 90° with the surface normal. The spectra were recorded for $\alpha = 30°$. They correspond to the traces indicated in Figure 7. The squares help to identify the spectra from the ω/k-diagrams given there.

spectra series in combination with right angle scattering experiments. The discrepancies between the wave numbers derived from the different spectra series can easily be realized from the two examples reproduced in Figs. 2 and 3 where the measured wave numbers are E(LO) 430/E(TO) 433 cm^{-1} and E(LO) 426/E(TO) 432 cm^{-1}, respectively.

The last more serious difference finally occurs on branch nr. 7, see Figure 4. The average information from the Raman spectra is an almost dispersion-free branch between E(TO) and E(LO) both at 371 cm^{-1}. This can be verified from Figs. 2 and 3. In none of the Raman spectra there was an indication that the LO-mode should be located at a much lower frequency. This stands drastically in contrast with the IR-experiments which suggest the assignment E(LO) 342 cm^{-1} and E(TO) 361 cm^{-1}. On the reflection spectra in Fig. 8 we observe the disappearance of a strong minimum at $\sim 350\ cm^{-1}$ when raising ϑ from 0° to 90°. The disappearance of this minimum can be explained only when the LO-frequency in question is located much lower at $\sim 342\ cm^{-1}$. Figure 7 clearly demonstrates this: compare the region of transparency around 350 cm^{-1} in the three figures. The results obtained from the two experimental methods here differ in principle. We believe that the solution of the problem is the following.

The Raman spectra show both ordinary and extraordinary phonons simultaneously. The IR-reflection experiments, however, are determined by the extraordinary modes only. The results obtained from these spectra therefore seem more reliable for our problem. The Raman spectra here obviously mainly show the directionally independent ordinary branch whereas the extraordinary one seems to exhibit too small scattering intensities.

A fit of the calculated directional dispersion branches to the experimental data was possible in both cases as can be seen from Figure 4. This seems somewhat unexpected at a first glance because the calculation is based only on the phonon data and the numerical values of the dielectric constants, see Equation (1). The values used of the latter were $\varepsilon_{\parallel}^{\infty} = 4.2$ for A_1-modes and $\varepsilon_{\perp}^{\infty} = 4.5$ for E-modes. These dielectric constants are of course known with a much higher accuracy as a function of frequency in the band gap from experiments [13]. The macroscopic theory for phonon polaritons as used hitherto, however, roughly approximates the influence of all exciton-states on the dispersion effects in the infrared by constant values ε_i^{∞} for the principal directions. This means that no frequency dependence of ε^{∞} is taken into account for large ω-values. The detailed experimental knowledge of the function $\varepsilon(\omega)$ in the band gap thus exceeds the possibilities of the present macroscopic polariton theory. For the future it therefore should be advantageous to include at least the lowest exciton polariton state in the theory of phonon-polaritons by a simple resonance term. This would make possible a fit of "$\varepsilon^{\infty}(\omega)$" in the band gap by choosing a suitable value of the exciton oscillator strength and thus eliminate the uncertainty in the choice of a constant ε^{∞}. Such calculations, however, would not bring any new information on $LiNbO_3$ at the present time. They might only confirm the fact that the FTR-method was superior to Raman-scattering experiments for the extraordinary branch 7, see above.

Acknowledgement

We want to thank Prof. J. Brandmüller for discussions and the Deutsche Forschungsgemeinschaft for financial support.

[1] R. Claus, L. Merten, and J. Brandmüller, Light Scattering by Phonon-Polaritons, Springer Tracts in Modern Physics, Vol. **75,** Springer-Verlag, Berlin 1975.
[2] W. G. Spitzer and D. A. Kleinman, Phys. Rev. **121,** 1324 [1961].
[3] J. F. Scott and S. P. S. Porto, Phys. Rev. **161,** 903 [1967].
[4] A. S. Barker and R. Loudon, Phys. Rev. **158,** 433 [1967].
[5] R. Claus, G. Borstel, E. Wiesendanger, and L. Steffan, Z. Naturforsch. **27 a,** 1187 [1972]; Phys. Rev. **B 6,** 4878 [1972].
[6] S. M. Shapiro and J. D. Axe, Phys. Rev. **B 6,** 2420 [1972].
[7] H. J. Falge, A. Otto, and W. Sohler, Phys. Stat. Sol. **(b) 63,** 259 [1974].
[8] W. Nitsch, H. J. Falge, and R. Claus, Z. Naturforsch. **29 a,** 1011 [1974].
[9] G. Borstel, H. J. Falge, and A. Otto, in Springer Tracts in Modern Physics **74,** 107 [1974].
[10] H. J. Falge, E. Schuller, and G. Borstel, Phys. Stat. Sol., to be published.
[11] V. A. Yakovlev, G. N. Zhizhin, M. I. Musatov, and N. M. Rubinina, Sov. Phys. Sol. State **17,** 1996 [1976].
[12] H. J. Falge, Dissertation, Munich 1974.
[13] G. D. Boyd, W. L. Bond, and H. L. Carter, J. Appl. Phys. **38,** 1941 [1967].